NJC

Accepted Manuscript

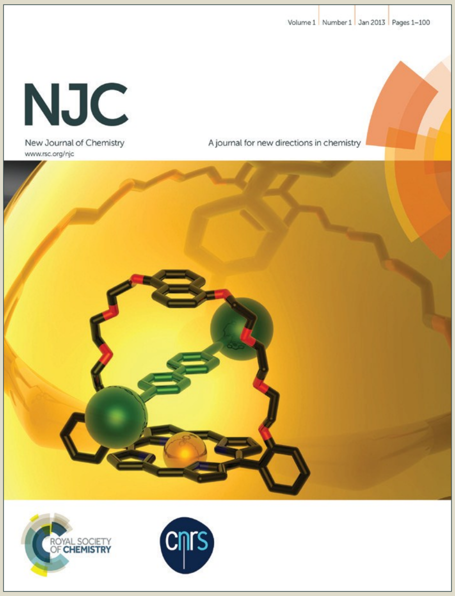

ROYAL SOCIETY OF CHEMISTRY

www.rsc.org/njc

NJC

PAPER

Preparation of multifunctional magnetic-fluorescent nanocomposites for analysis of tetracycline hydrochloride

Received 00th January 20xx,
Accepted 00th January 20xx

DOI: 10.1039/x0xx00000x

www.rsc.org/

Xiaowan Li,[1] Chenyu Li[2] and Ligang Chen[1,*]

A multifunctional nanocomposites for highly sensitive and rapid detection of tetracycline hydrochloride (TC), has been developed using magnetic quantum dots (MQDs). The thiolated quantum dots (QDs) was conjugated on the amino-coated Fe_3O_4 and crosslinking modification with EDC/NHS through covalent binding. The obtained MQDs possess superparamagnetic behavior, fluorescence properties and exhibit a strong orange metal-to-ligand charge transter emission. The MQDs were characterized by fluorescence spectrophotometry, X-ray powder diffraction, Fourier transform infrared spectroscopy, physical property measurement system and transmission electron microscope. The multifunctional nanomaterial shows excellent fluorescence properties that allow for highly sensitive and short response time for TC detection. Under optimum conditions, a linear calibration plot of the quenched fluorescence intensity at 593 nm against the concentration of TC was observed range from 10 to 700 nmol L^{-1} with a detection limit of 1.2 nmol L^{-1} is obtained. The recovery detected with this method was from 95.7% to 99.3% with a relative standard deviation (R.S.D.) below 3%. This method manifested several advantages such as high sensitivity, non-toxic, short analysis time, low cost and ease of operation.

1. Introduction

Tetracycline hydrochloride (TC) is a broad-spectrum antibiotic which can be used in the treatment of disease caused by gram-negative and gram-positive microorganisms and so on.[1] The chemical structure of TC is shown in Fig. 1. Besides its antibiotics property, it can also affect immunomodulation, angiogenesis, inflammation and cell proliferation.[2] Moreover, during past decades, this medicine has been widely used as a model drug for the research of drug delivery system.[3] Large dosage can lead to increased drug resistance of microbial strains in human beings and cause allergic or toxic reactions among some hypersensitive individuals.[4]

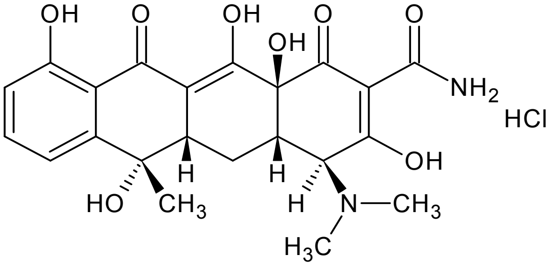

Fig. 1 Chemical structure of tetracycline hydrochloride.

To our knowledge, TCs are usually determined by high-performance liquid chromatography (HPLC),[5] capillary electrochromatography,[6] microbiological analysis,[7] electro-chemical analysis,[8] immune assay,[9] fluorimetric method,[10] photoluminescence detection,[11] surface plasmon resonance spectroscopy,[12] titrimetry,[13] and voltammetric analysis.[14] Each method has distinct advantages and drawbacks. For example, chromatographic methods are sensitive, but time consuming and dependent on highly skilled personnel and expensive equipment. Principal disadvantages of immune methods are their frequent high background, and complicated sample handling procedure. Thus, they are not suitable for routine, large scale screening. Other methods mentioned above are either time consuming or not suitable for field analysis. Thus, high sensitivity, short analysis time, low cost and ease of operation methods are required for fluorometric analysis of TC. Among the various reported techniques, fluorescence analysis presents many appealing advantages, including high sensitivity, economical, rapid, and easy detection.

Nowadays, QDs are a brand new class of fluorescent nanoprobes, the semiconductor particles have all three dimensions confined to the 2-10 nm length scale.[15] As special semiconductor nanoclusters,[16] QDs have generated a tremendous amount of interests owing to their unique optical properties, such as broad excitation spectra, narrow tunable and symmetric emission spectra as well as excellent photostability.[17] QDs have applied to the determination of paeonol,[18] roxithromycin,[19] ascorbic acid,[20] sulfadiazin.[21] These studies reveal that the interactions between some substances and the QDs would change their photophysical properties.

---

[1] *Department of Chemistry, College of Science, Northeast Forestry University, 26 Hexing Road, Harbin 150040, China*

[2] *Center of Disease Control of Heilongjiang Province, 40 Youfang Street, Harbin 150030, China.*

E-mail: ligangchen2008@163.com (L. Chen); Tel: +86-451- 82190679-8244

ZnS:Mn QDs have attracted great interest on account of their high quantum efficiency and thermal stability, essential properties for chemical applications such as chemical and biosensor, molecular imaging, monitoring drug delivery, etc.[22,23]

Recently, the progress in controlled synthesis of high-quality QDs, as well as the effective surface modifications have intrigued analytical chemists to explore QDs as promising optical labels for sensing and biosensing events. QDs have attracted considerable attention due to sensitive and simple sensors as novel luminescence probes in the detection of drug. But tedious centrifugal process is inevitable, which will increase the nano-particles agglomeration. So the analyzing result is existed some certain errors. In order to overcome these drawbacks effectively, the MQDs technique has been developed.

Recently, Fe_3O_4 based on particles has been of intense interest in the research of sample pretreatment due to their ease of preparation and surface modification, ease of operation, and excellent dispersibility in aqueous solution.[24] Magnetic particles with special functionalities bound onto the surface could be applied to enrichment analytes, and it can be easily and quickly isolated by applying an external magnetic field placed outside the enrichment container. So the analytes could be separated rapidly from large-volume samples, and avoided the difficulties of solid-liquid separation.

Among so many appealing functionalities, magnetism and fluorescence attract more attention due to their individual advantages.[25] In this context, appropriate combination of both functionalities into a single entity will complement each other, leading to more powerful tools for applications. For this reason, much effort has been devoted to the elaboration of magnetic-fluorescent nanocomposites, such as magnetic QDs.[26] MQDs can be employed to separate and enrich the analytes from complicated samples, and then the enriched analytes can be detected with the fluorescent signal generated by MQDs. Recently, interest in nano-scaled magnetic particles is increased because of their potential applications in many fields especially in the pharmaceutical industry for targeted drug delivery. Nano-magnetite particles are easily obtained through various chemical synthetic techniques and easily separated from solution by an external magnetic field.

In the present work, the aim was to develop a novel and rapid method for determination of TC. We demonstrate a very simple and effective method to prepare magnetic QDs with good optical properties and magnetic properties. In this method, 3-aminopropyl triethoxysilane (APTES) and thioglycolic acid (TGA) were used to control the aggregation of Fe_3O_4 and QDs, respectively. Moreover, Fe_3O_4 and QDs were conjugated through the reaction between amino group and carboxylic group. The characteristics of the MQDs were investigated by fluorescence spectrophotometry, X-ray powder diffraction, Fourier transform infrared spectroscopy, physical property measurement system and transmission electron microscope. The preconcentration process of TC sample was optimized to obtain satisfactory recoveries of TC sample. Good recovery and precision with low detection limit were obtained. As mentioned above, these magnetic-fluorescent nanocomposites with water-dispersibility, good magnetic response, fluorescence probe property would have potential application in pharmaceutical analysis.

2. Experimental

2.1 Reagents and chemicals

The standard of tetracycline hydrochloride (TC) (99.99%) was purchased from Aladdin (Shanghai, China). Zinc sulfate heptahydrate ($ZnSO_4$ • 7H2O) (⩾ 99.5%) was purchased from Shuangchuan (Tianjin, China). Manganese (II) chloride tetrahydrate ($MnCl_2$ • $4H_2O$) (⩾ 99.0%) was purchased from Bodi (Tianjin, China). Sodium Sulfide (Na_2S • $9H_2O$) (⩾ 98.0%) was purchased from Kaitong (Tianjin, China). Ferric chloride ($FeCl_3$ • $6H_2O$) (⩾ 99.0%) was purchased from Zhiyuan (Tianjin, China). Thioglycolic acid (TGA) (90.0%), 1-ethyl-3-[3-dimethylaminopropyl] carbodiimide hydrochloride (EDC) (98.5%), N-hydroxysuccinimide (NHS) (98.0%), 3-aminopropyltriethoxysilane (APTES) (98.0%) and Iron (II) chloride tetrahydrate ($FeCl_2 \cdot 4H_2O$) were purchased from Aladdin (Shanghai, China). Ethanol and sodium hydroxide (NaOH) were obtained from Kermel (Tianjin, China). Three tetracycline hydrochloride tablets samples were collected from Harbin (China) pharmacy. All reagents were at least of analytical grade. High-purity water was obtained from a Milli-Q water system (Millipore, Billerica, MA, USA).

2.2 Apparatus

Fourier transform infrared (FT-IR) spectrum of the MQDs was recorded with FT-IR360 spectrometer (Nicolet, Madison, WI, USA) using KBr method. The X-ray powder diffraction (XRD) spectrum was collected on a Shimadzu XRD-600 diffractometer (Kyoto, Japan) with Cu Kα radiation. The morphology of magnetic QDs was observed with a transmission electron microscope (TEM) (H7650, Matsudo, Japan). Fluorescence intensity studies were carried out at room temperature by using Perkin-Elmer LS-55 fluorescence spectrometer (Maryland, USA) which was equipped with a plotter unit and a quartz cell. Magnetic properties were measured by a physical property measurement system (PPMS) (Quantum Design Instrument, San Diego, CA, USA). A KQ5200E ultrasonic apparatus (Kunshan Instrument, Kunshan, China) was used for making samples dispersed evenly.

2.3 Preparations of Fe_3O_4 @ ZnS:Mn^{2+} QDs

The synthesis of Fe_3O_4 nanoparticles capped with APTES was based on the reported method with a little modification.[27] As follows: 0.01 mol $FeCl_2 \cdot 4H_2O$ and 0.02 mol $FeCl_3 \cdot 6H_2O$ were dissolved in 100 mL of water. The mixture was stirred vigorously and purged with nitrogen gas. When the temperature increased to 80 °C, 40 mL of NaOH solution (2.0 mol L^{-1}) was added into the mixture. After 1.0 h, the magnetic precipitates were isolated from the solvent by a permanent magnet and washed several times with water. The Fe_3O_4 nanoparticles (25 mg) were dispersed in ethanol (25mL), and then APTES (0.1mL) was added into it. The mixture was stirred at 300 rpm for 24 h at room temperature. After completion of reaction, the reaction mixture was isolated from the solvent by a permanent magnet and washed several times with water.

The synthesis method of Mn-doped ZnS QDs was shown as follows.[28] At first, 25 mmol of $ZnSO_4{\cdot}7H_2O$, 2 mmol of $MnCl_2{\cdot}4H_2O$ and 80 mL water were kept stirring for 20 min under the protection of nitrogen gas. Then, 25 mmol $Na_2S{\cdot}9H_2O$ (10 mL) solution was added drop wise into the mixture. After being stirred for 30 min, 4 mL of TGA was added for modifying the Mn-doped ZnS QDs by magnetic stirring for 12 h at room temperature. Finally, the modified Mn-doped ZnS QDs was obtained after centrifugation and being washed with ethanol three times.

APTES-modified Fe_3O_4 (5.0 mg), TGA-modified Mn-doped ZnS QDs (30 mg), EDC (5.0 mg) and NHS (5.0 mg) were dispersed in 20 mL water by ultrasonic. The mixture of Fe_3O_4 and QDs were stirred for 30 min and placed in dark places for 10 h at room temperature. The MQDs were washed with water three times, dispersed in water and seal paced in the refrigerator.

2.4 Fluorescence analysis

Fluorescence analysis was performed on Perkin Elmer LS-55 fluorescence spectrometer. The spectra were recorded in the wavelength range of 350-750 nm upon excitation at 300 nm. Slit widths (10 nm), scan speed (200 nm min^{-1}) and excitation voltage (750 V) were kept constant within each data set and each spectrum was the average of three scans. Quartz cell (1 cm path length) was used for all measurements.

2.5 Measurement of fluorescent response to TC

The resulting 1.5 mg MQDs were added to 300 mL TC sample solution. The mixture was stirred at room temperature for 8 min with stirring rate of 300 r/min. The magnetic nanoparticles were isolated rapidly from the solution by applying an external magnetic field. After dis-carding the supernatant solution, the solid was dispersed in water, the solution pH was adjusted to 8.0. The pre-concentration factors achieved were 100 through separating solid adsorbed with analyte from 300 mL aqueous solution and dispersing to a final volume of 3.0 mL. Then, the fluorescence intensity of MQDs adsorbed with TC was measured. The TC tablets samples were applied to evaluate the practical application. The recovery study was carried out by spiking certain volume of TC solution into tablets samples.

3. Results and discussion

3.1 Characterization of MQDs

We synthesized superparamagnetic nanoparticles modified with surface amination. Moreover, QDs were modified with TGA which served two major purposes: firstly, it rendered the hydrophobic QDs hydrophilic through surface modification, which was an essential prerequisite for their applications; secondly, the free carboxyl groups, introduced by TGA, made the QDs available for further conjugation. By using the EDC/NHS chemistry, preparation of MQDs was achieved through the covalent binding interactions between the amino groups of APTES-capped Fe_3O_4 and the carboxylic groups on the surface of TGA-capped ZnS:Mn^{2+} QDs.[29]

3.2 Fluorescence properties of MQDs

The optical properties of ZnS:Mn^{2+} QDs and Fe_3O_4@ZnS:Mn^{2+} QDs are investigated with fluorescence spectra (Fig. 2). The fluorescence intensity of the magnetic QDs was recorded by varying the excitation wavelength from 300 to 350 nm and was shown in the weak blue peak around 444 nm was generated by the defect related to the emission of the ZnS QDs. The maximum emission intensity at 593 nm was observed with the excitation wavelength at 300 nm. The strong orange peak around 593 nm could be attributed to the $^4T_1 \rightarrow {}^6A_1$ d-d transition of Mn^{2+} ions on Zn^{2+} sites, where Mn^{2+} is tetrahedrally coordinated by S^{2-}. This can be explained as Mn^{2+} incorporated into the ZnS lattice led to the Mn^{2+} based orange emission while ZnS with surface bound Mn^{2+} yielded the ultraviolet emission.[30,31]

When the QDs doped with Fe_3O_4, their fluorescence intensity was decreased. However, it is enough to analyze TC by fluorescence quenching method. MQDs have the advantages of rapid separation and enrichment of analytes.

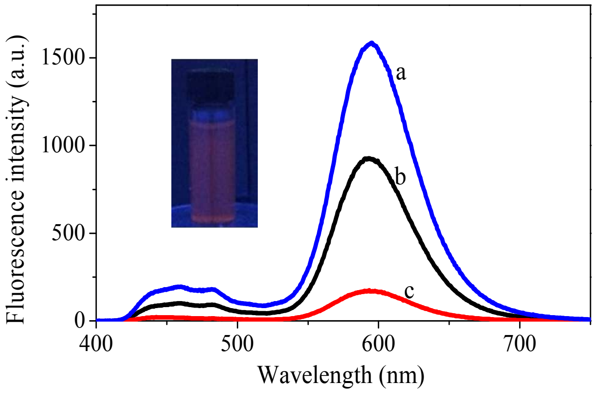

Fig. 2 Fluorescence spectra of TGA-capped ZnS:Mn^{2+} QDs (0.5 mg mL^{-1}, pH 8.0) (a) and Fe_3O_4@ZnS:Mn^{2+} QDs (0.5 mg mL^{-1}, pH 8.0) in the absence (b) and presence (c) of TC (700 nmol L^{-1}), the inset shows the photographs of MQDs under UV illumination.

Fig. 2c shows the fluorescence quenching of Fe_3O_4@ZnS:Mn^{2+} QDs upon interaction with TC. Inset of Fig. 2 shows photograph of an aqueous dispersion of Fe_3O_4@ZnS:Mn^{2+} QDs under UV illumination. The MQDs may be excited with ultraviolet light (300 nm), and the emitted fluorescence (593 nm) is quenched by TC. This quenching process could be readily monitored, and given an appropriate set of calibration samples, would result in a method for quantitative analysis of TC.

3.3 Characterization of the synthesized MQDs

TEM and XRD of Fe_3O_4@ZnS:Mn^{2+} QDs were shown in Fig. 3 and Fig. 4, respectively. TEM image shows that the size of the MQDs sample is in the range of about 30 nm with almost spherical particles. In order to investigate the crystalline structure and purity of nanoparticles, XRD spectrum was performed on the Fe_3O_4 nanoparticles, ZnS:Mn^{2+} QDs and the magnetic QDs. The typical peaks of Fe_3O_4 at 2θ = 30.3°, 35.4°, 43.1°, 57.4° and 62.4° are observed (Fig. 4a). The diffractions at 28.6°, 48.5° and 56.8° reflect the characteristic of (111), (220), and (311) planes of cubic zinc blende nanoparticles (Fig. 4b).[32] The peaks are broadened because of the finite crystalline size. The X-ray data in Fig. 4c could be consistent with the composite structure of Fe_3O_4 and ZnS:Mn^{2+} QDs.

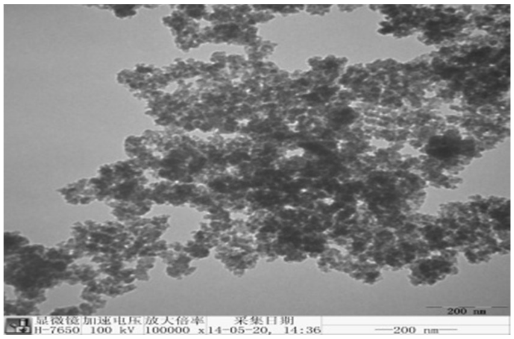

Fig. 3 Representative TEM image of magnetic QDs.

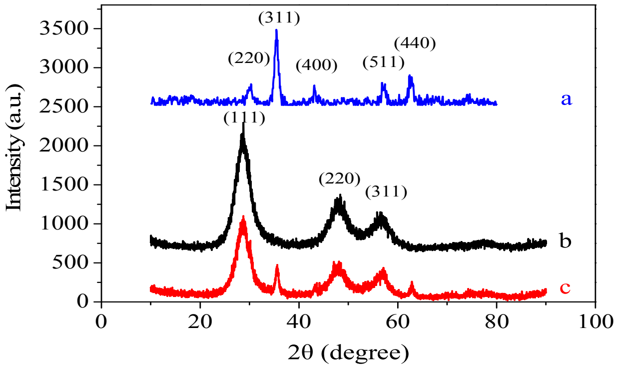

Fig. 4 XRD patterns of Fe_3O_4 (a), ZnS:Mn^{2+} QDs (b) and Fe_3O_4@ZnS:Mn^{2+} QDs (c).

The FT-IR spectrum of magnetic QDs was given in Fig. 5. The peak located at 570 cm^{-1} is the characteristic band of Fe_3O_4. The peak at 3413 cm^{-1} might originate from the stretching vibration of O-H bond. The adsorption band at 1565 cm^{-1} indicated the successful introduction of amino groups onto the surface of magnetic QDs, which is due to APTES bonded to the magnetic QDs. Peaks at 1384 and 1616 cm^{-1} represents C-N and C=O stretching vibration, respectively. Results showed that the stretching band of the S-H thiol group, 2550-2670 cm^{-1} S-H, is not observed when the nanoparticles are evaluated. The reason for disappearance of S-H group vibration on the surface of ZnS QDs is due to the formation of covalent bonds between thiols and Zn^{2+} surface atoms.[33]

To examine the magnetic properties, the nano-particles were studied by PPMS at room temperature. The saturation magnetization of magnetic QDs decreased to 23.2 emu g^{-1} from 59.6 emu g^{-1} of Fe_3O_4. As shown in Fig. 6 (inset), in the

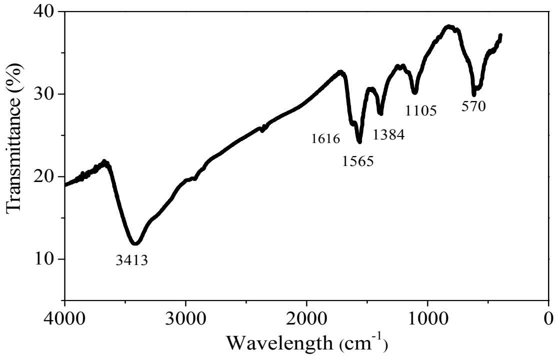

Fig. 5 FT-IR spectrum of Fe_3O_4@ZnS:Mn^{2+} QDs.

presence of an external magnetic field, the magnetic QDs were attracted to the wall of vial, in comparison with a brown homogeneous dispersion existed without an external magnetic field. The as synthesized adsorbent dispersed in water can be easily collected by external magnetic field in a short time (Fig. 6), and then can be readily re-dispersed with slightly shake.

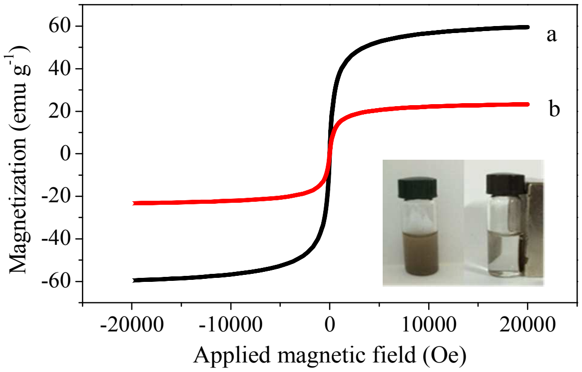

Fig. 6 Magnetization curves of the Fe_3O_4 (a) and the Fe_3O_4@ZnS:Mn^{2+} QDs (b). The inset shows the magnetic separation photographs of Fe_3O_4@ZnS:Mn^{2+} QDs under permanent magnet.

3.4 Effect of pH on the fluorescence intensity of Fe_3O_4@ZnS:Mn^{2+} QDs

For the consistent and efficient utilization of QDs in pharmacological application, it is necessary to understand the factors that affect the optical behavior of QDs. To test the influence of pH on the fluorescence intensity of the prepared Fe_3O_4@ZnS:Mn^{2+} QDs, we kept the concentration of Fe_3O_4@ZnS:Mn^{2+} QDs constant and varied the pH values ranging from 3 to 12 (Fig. 7). The pH dependence observed clearly reveals that the intensity of Fe_3O_4@ZnS:Mn^{2+} QDs significantly enhanced as the pH was changed from 3 to 8 and reaches a maximum at pH 8 and then decreased when pH value continuously increased.

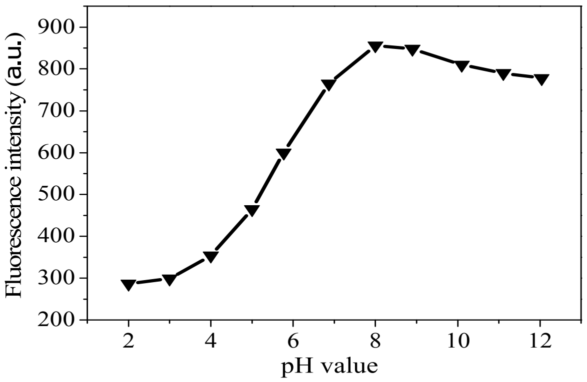

Fig. 7 Effect of pH on the fluorescence of $Fe_3O_4@ZnS:Mn^{2+}$ QDs.

3.5 Effect of reaction time

In order to validate the reaction time, the fluorescence intensity of a typical mixing of $Fe_3O_4@ZnS:Mn^{2+}$ (0.5 mg mL^{-1}) and TC solution (700 nmol L^{-1}) were studied at maximum emission wavelength (λ_{em} = 593 nm, λ_{ex} =300 nm), under optimum condition. The influence of incubation time on the fluorescence intensity investigated at different time scales was shown in Fig. 8. It was found that the mixture showed a rapid decrease in fluorescence intensity after the TC added. The reaction was completed within 8 min at room temperature, and the fluorescence intensity remained constant for 1 h. Therefore, the experiments were carried out after 8 min and the time scale of 8 min was also adopted in the following experiments.

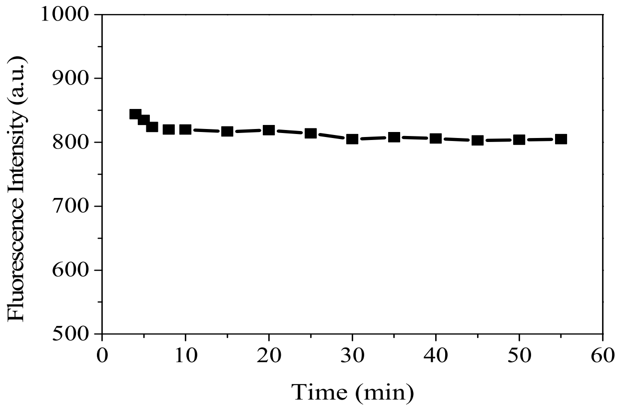

Fig. 8 Influence of incubation time on the fluorescence quenching reaction between $Fe_3O_4@ZnS:Mn^{2+}$ QDs and TC.

3.6 Fluorescence detection of TC based on $Fe_3O_4@ZnS:Mn^{2+}$ QDs

Fig. 9a shows the fluorescence quenching of $Fe_3O_4@ZnS:Mn^{2+}$ QDs upon interaction with different concentrations of TC for a fixed interval time of 8 min under the optimal conditions mentioned above. The influence of concentrations of magnetic $ZnS:Mn^{2+}$ QDs on quenching measurement were investigated. In order to optimize the concentrations of QDs to probe TC, a various concentration ranging from 10 to 700 nmol L^{-1} were added. The result shown in Fig. 9a illustrates that when the concentrations of magnetic QDs increased, the F_0/F also increases. F_0 and F are the fluorescence intensity of magnetic QDs in the absence and presence of a quencher (TC), respectively.

As the concentration of TC increased, the quenching of magnetic QDs was enhanced. Calibration curve in Fig. 9b was the plots of the optical analysis at different concentrations of TC by the quenching of the emission maximum of $Fe_3O_4@ZnS:Mn^{2+}$ QDs. The results exhibited a good linear relationship range from 10 to 700 nmol L^{-1}. The limit of detection is defined by $3\sigma/K$, where σ is the standard deviation of blank measurements (n = 11) and K is the slope of calibration graph, the detection limit was 1.2 nmol L^{-1}. Compared with some methods such as HPLC, capillary electrophoresis, micellar electrokinetic chromatography, which have reported before, the detection limit of this method is lower and high sensitivity, this method is characterized by simplicity, low consumption and rapidity.

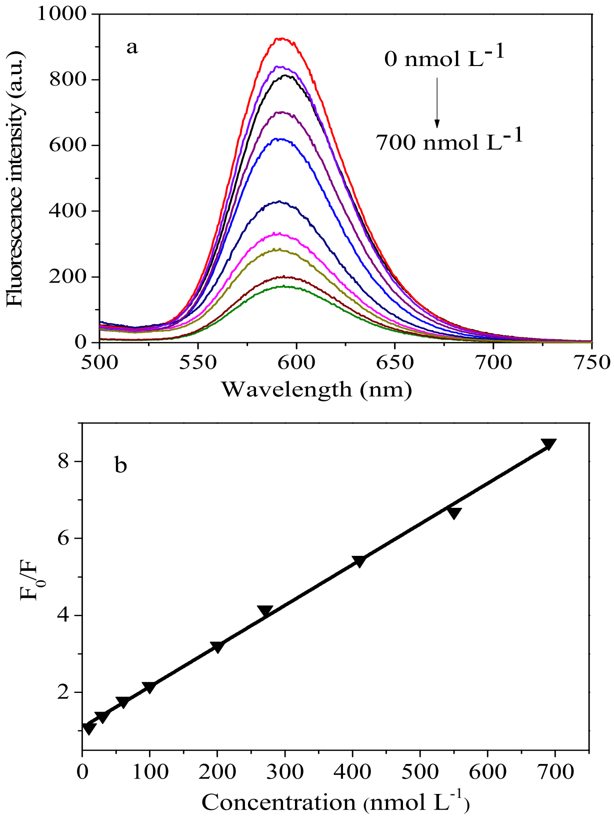

Fig. 9 Fluorescence spectra of $Fe_3O_4@ZnS: Mn^{2+}$ QDs (λ_{ex} =300 nm) with TC various concentration ranging from 0 to 700 nmol L^{-1} (a) and the linear plots of the quenched fluorescence intensity of $Fe_3O_4@ZnS: Mn^{2+}$ QDs against the concentration of TC (b) with a 0.9989 correlation coefficient.

3.7 Mechanism of magnetic QDs for the detection of TC

The fluorescence intensity of $Fe_3O_4@ZnS:Mn^{2+}$ QDs reduced with the addition of TC. Fluorescence quenching mechanism generally falls into two kinds, dynamic quenching and static quenching. Dynamic and static quenching can be distinguished by their differing dependence on temperature. For dynamic quenching, the quenching constants increase with the increase of temperature, whereas the crosscurrent is observed in the case of static quenching. The quenching mechanism of TC on the fluorescence of magnetic QDs could be revealed by the well-known Stern–Volmer equation:[34]

$$F_0 / F = 1 + K_{SV}[Q] \quad (1)$$

In this expression, F_0 and F are the fluorescence intensity of magnetic QDs in the absence and presence of a quencher (TC), respectively; $[Q]$ is the concentration of the quencher; K_{SV} is the Stern–Volmer dynamic quenching constant that indicates the quenching efficiency of the quencher.

In Fig. 10, the fluorescence quenching mechanism can be analyzed at different temperatures (293 K, 303 K and 313 K) with the Stern–Volmer equation.[35] We have calculated the TC of the magnetic QDs system at three different temperatures according to equation 1 and showed them in Table 1. It can be seen that the quenching constant increase with the rise of temperature, which indicate that the probable quenching mechanism of magnetic QDs solution system is dynamic quenching.

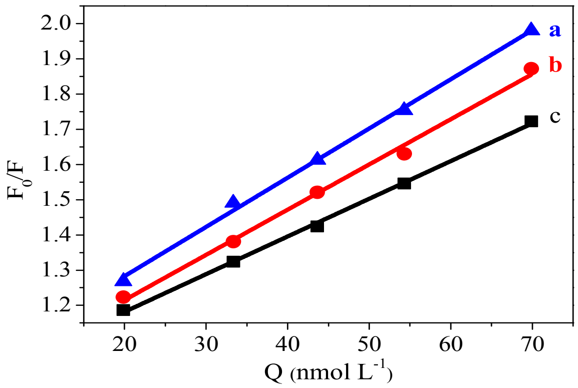

Fig. 10 Stern-Volmer curves for the Fe_3O_4@ZnS: Mn^{2+} QDs with TC solution system at three different temperatures (a. 313K; b. 303K and c. 293K).

The enthalpy change (ΔH^o), free enthalpy change (ΔG^o), and entropy change (ΔS^o) were calculated according to the following thermodynamic equations:

$$\Delta G^o = -RT \ln K_{SV} \quad (2)$$

$$\Delta G^o = \Delta H^o - \Delta S^o T \quad (3)$$

By rearranging the equations 2 and 3, K_{SV} may be calculated using the following relationship

$$\ln K_{SV} = \frac{\Delta S^o}{R} - \frac{\Delta H^o}{RT} \quad (4)$$

where R is the universal gas constant (8.314 J mol^{-1} K^{-1}) and T is the quenching temperature in Kelvin. K_{SV} is the equilibrium constant at the corresponding temperature, which stands for quenching constant. The values of ΔG^o (kJ mol^{-1}), ΔH^o (kJ mol^{-1}) and ΔS^o (J mol^{-1} K^{-1}) are presented in Table 1. The values of ΔG^o were negative at all temperatures, confirming that the quenching of TC onto magnetic QDs was spontaneous andthermodynamically favorable. ΔH^o suggested an endothermic quenching, which was supported by the observation that the quenching of TC onto magnetic QDs increased with increasing quenching temperature (in Table 1).

Table 1

Thermodynamic parameters of Fe_3O_4@ZnS: Mn^{2+}-TC system.

T (K)	K_{sv} (L mol^{-1})	ΔG^o (kJ mol^{-1})	ΔH^o (kJ mol^{-1})	ΔS^o (J mol^{-1} K^{-1})
293	1.07×10^5	-28.21	13.103	141
303	1.28×10^5	-29.62		
313	1.40×10^5	-30.84		

3.8 Interference of co-existing foreign substances

To explore the selectivity of this method using magnetic quantum dots as probe for the determination of TC solution. In order to investigate the possibility of practical application of the procedure, the interference from some familiar metal ions, inorganic anions and biomolecules were tested under the optimum conditions. From the results displayed in Table 2, we can see that most of the common metal ions, glucide, amino acids and common inorganic cation could be allowed at high concentration. The method has good selectivity.

Table 2

Effects of coexistent substances of MQDs-TC solution system. (pH, 8; TC,70 nmol L^{-1})

Coexistence materials	Concentration (μmol L^{-1})	Relative Error (%)
K^+	100	+ 1.25
Na^+	100	+ 1.03
Mg^{2+}	100	+ 0.90
Al^{3+}	50	- 1.32
Ca^{2+}	10	- 1.61
Pd^{2+}	10	- 4.15
Cu^{2+}	10	- 3.47
Cd^{2+}	10	- 1.83
NH_4^+	50	+ 2.60
Cl^-	100	+ 1.05
NO_3^-	80	- 2.56
CO_3^{2-}	50	+ 1.96
Urea	10	+ 3.07
Glucose	5	+ 3.50
Lactose	5	+ 3.86
Sucrose	5	- 3.75
Maltose	5	- 1.76
Lactamine	5	+ 3.04
Tryptophan	5	+ 1.90
Histidine	5	+ 2.07
Glycine	5	+ 1.85
Amylum	500	- 2.28

3.9 Analytical application

To evaluate the applicability and validity of this newly propose sensor for the determination of TC, this method was applied to determine TC in commercial pharmaceutical dosage forms (tablet). The tablets were handled according to previous report[36] with minor modification. The results show that the average content of TC from replicate measurements was 317 nmol L^{-1}. Recovery experiments were performed by using the standard addition method. Complete results of this analysis were an acceptable recovery range from 95.7 to 99.3%, and the relative standard deviation (RSD) ranged from 1.9% to 2.7%, these values indicated that this method had good accuracy and precision for quantitive determination of TC in the presence of excess amount of other substances, indicating that the determination of tetracycline hydrochloride using magnetic QDs as fluorescence probe was high sensitive and reliable.

4. Conclusions

In conclusion, we have established a rapid and sensitive method which used the change of fluorescence intensity of magnetic quantum dots to detect the content of tetracycline hydrochloride. The preparation of Fe_3O_4@ZnS:Mn^{2+} quantum dots is simple and inexpensive. The Mn-doped ZnS quantum dots and Fe_3O_4 were conjugated by the condensation reaction between -COOH and -NH_2 with adding 1-ethyl-3-[3-dimethylaminopropyl] carbodiimide hydrochloride and N-hydroxysuccinimide. Under optimum conditions, the calibration plot was linear in the concentration range from 10 to 700 nmol L^{-1} with detection limit of 1.2 nmol L^{-1} and a correlation coefficient (*R*) of 0.9989. Based on the results, the designed sensor can be used to detect the tetracycline hydrochloride with good sensitivity, other advantages of include its simplicity, rapidity, highly selectivity over other substance. The fluorescent, magnetic, and water-soluble properties of magnetic quantum dots nanoparticles would allow them to find applications in biolabeling, bioseparation, diagnostics fields and pharmaceutical analysis.

Acknowledgements

This work was supported by the Fundamental Research Funds for the Central Universities (No.2572014EB06) and Heilong Jiang Postdoctoral Funds for scientific research initiation (No.LBH-Q14001).

References

1 I. Chopra and M. Roberts, *Microbiol. Mol. Biol. R.*, 2001, **65**, 232–260.
2 F. Alava-Moreno, Y. M. Liu, M. E. Díaz-García and A. Sanz-Medel, *Microchim. Acta*, 1993, **112**, 47-54.
3 E. R. Kenawy, G. L. Bowlin, K. Mansfield, J. Layman, D. G. Simpson, E. H. Sanders, and G. E. Wnek, *J. Control. Release*, 2002, **81**, 57-64.
4 J. A. Rodriguez, J. Espinosa, K. Aguilar-Arteaga, I. S. Ibarra and J. M. Miranda, *Microchim. Acta*, 2010, **171**, 407-413.
5 D. S. Aga, S. O'Connor, S. Ensley, J. O. Payero, D. Snow and D. Tarkalson, *J. Agr. Food Chem.*, 2005, **53**, 7165–7171.
6 J. L. Chen and K. H. Hsieh, *Electrophoresis*, 2010, **31**, 3937-3948.
7 M. G. Pikkemaat, *Ana.l Bioanal. Chem.*, 2009, **395**, 893-905.
8 Y. J. Kim, Y. S. Kim and J. H. Niazi, *Bioproc. Biosyst. Eng.*, 2010, **33**, 31-37.
9 T. Le, H. Yu, Z. W. Zhao and W. Wei, *Anal. Lett.*, 2012, **45**, 386–394.
10 K. W. Kohn, *Anal. Chem.*, 1961, **33**, 862–866.
11 J. M. Traviesa-Alvarez, J. M. Costa-Fernández, R. Pereiro and A. Sanz-Medel, *Anal. Chim. Acta*, 2007, **589**, 51–58.
12 M. Frasconi, R. Tel-Vered, M. Riskin and I. Willner, *Anal. Chem*., 2010, **82**, 2512–2519.
13 S. A. Nabi, E. S. M. Abu-Nameh and M. I. H. Helaleh, *J. Pharmaceut. Biomed.*, 1998, **17**, 357–359.
14 P. Masawat and J. M. Slater, *Sensor. Actuat. B-Chem.*, 2007, **124**, 127–132.
15 C. J. Murphy, *Anal. Chem.*, 2002, **74**, 520A–526A.
16 S. Kanwal, X. H. Fu and X. G. Su, *Microchim. Acta*, 2010, **169**, 167-172.
17 W. C. W. Chan and S. M. Nie, *Science*, 1998, **281**, 2016-2018.
18 W. Dong, H. B. Shen, X. H. Liu, M. J. Li and L. S. Li, *Spectrochim. Acta A*, 2011, **78**, 537-542.
19 J. Y. Peng and X. Y. Hu, *J. Lumin.*, 2011, **131**, 952-955.
20 S. S. Yang, C. L. Ren, Z. Y. Zhang, J. J. Hao, Q. Hu and X. G. Chen, *J. Fluoresc.*, 2011, **21**, 1123-1129.
21 M. M. Liu, L. Xu, W. Q. Cheng, Y. Zeng and Z. Y. Yan, *Spectrochim. Acta A*, 2008, **70**, 1198-1202.
22 Y. Shang, L. Qi, F.Y. Wu, *Microchim. Acta,* 2012, **177**, 333-339.
23 T. Zhao, X. Hou, Y.N. Xie, L. Wu, P. Wu, *Analyst,* 2013, **138**, 6589-6594.
24 H. Chen, C. Deng, X. Zhang, *Angew. Chem. Int. Ed. Engl,* 2010, **49**, 607-611.
25 A. Quarta, R. D. Corato, L. Manna, A. Ragusa and T. Pellegrino, *Ieee T. Nanobiosci.*, 2007, **6**, 298–308.
26 Y. Xu, A. Karmakar, D. Y. Wang, M. W. Mahmood, F. Watanabe, Y. B. Zhang, A. Fejleh, P. Fejleh, Z. R. Li, G. Kannarpady, S. Ali, A. R. Biris and A. S. Biris, *J. Phys. Chem. C*, 2010, **114**, 5020-5026.
27 G. Z. Li, W. C. Peng, X. Y. Li, X. B. Fan, X. J. Li, G. L. Zhang and F. B. Zhang, *Appl. Surf. Sci.*, 2008, **254**, 4970–4979.
28 J. X. Liu, H. Chen, Z. Lin and J. M. Lin, *Anal. Chem.*, 2010, **82**, 7380-7386.
29 X. P. Wei, T. Liu, T. Y. Qu and J. P. Li, *Chinese J. Instrum. Anal.*, 2012, **31**, 332-336.
30 A. A. Bol and A. Meijerink, *J. Lumin.*, 2000, **87–89**, 315-318.
31 R. Beaulac, P. I. Archer, D. R. Gamelin, *J. Solid State Chem.,* 2008, **181**, 1582-1589.
32 R. Kripal, A. K. Gupta, S. K. Mishra, R. K. Srivastava, A. C. Pandey and S. G. Prakash, *Spectrochim. Acta A*, 2010, **76**, 523-530.
33 S. N. Azizi, M. J. Chaichi, P. Shakeri and A. Bekhradnia, *J. Lumin.*, 2013, **144**, 34-40.
34 O. R. Quayle, *Chem. Rev.*, 1953, **53**, 439-589.
35 S. Kasai, T. Horie, T. Mizuma and S. Awazu, *J. Pharm. Sci.*, 1987, **76**, 387-392.
36 J. Tjørnelund and S. H. Hansen, *J. Chromatogr. A*, 1996, **737**, 291-300.

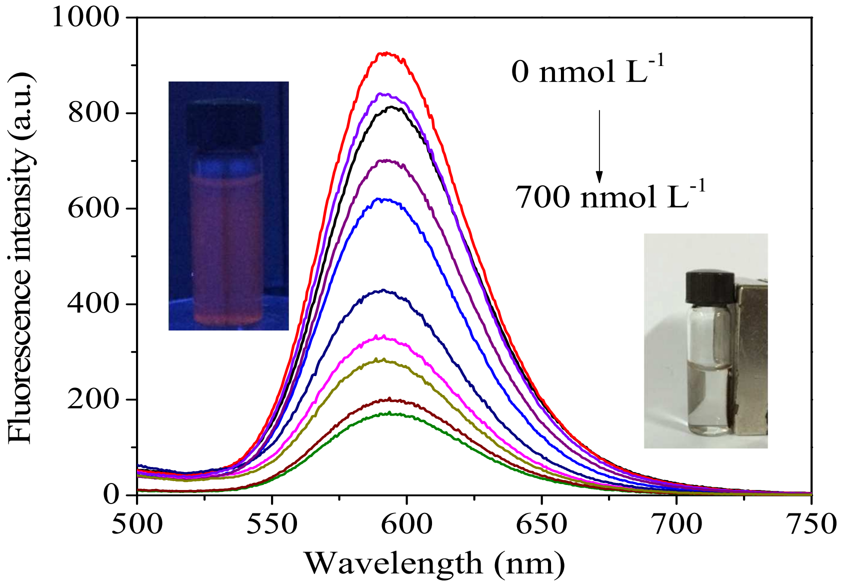

Magnetic quantum dots were effective material for detection of tetracycline hydrochloride with various concentrations.